necessarily exist, as it is indicated by stress relaxation. A number of general conclusions may be drawn from Eqs. (18) and (16).

1) To have $X(t)$ periodic for periodically varying external pressure, i.e., to make the integrals in Eq. (18) vanish at time $t_\lambda = 2\lambda\pi/\omega$ ($\lambda = 1,2,3,\ldots$) would imply the drastic linearization in Eq. (18)

$$(p/p_c)^3(1-p/p_c)^{-1} \sim (p/p_c)^3(1-p/p_c)^{-3} \sim (p/p_c)^3$$

Therefore, periodically varying external pressure cannot correspond to a periodic shape factor.

2) In general, for time-varying external pressure there exists a critical time t_{cr}, for which the shape factor will increase indefinitely large. This critical time is then a functional of the external loading, defined by

$$\int_0^{2\tau_c^{-1}t_{cr}} \left(\frac{p/p_c}{1-p/p_c}\right)^3 \exp\left(\int_0^v \frac{(p/p_c)^3}{1-p/p_c}du\right)dv = 9/2X_{oo}^2 \qquad (22)$$

where $u = 2\tau_c^{-1}\xi$ has been substituted in Eq. (18) and $p(\xi)$ has been transformed to $p(u)$.

3) The critical time is shortened when symmetrical pulsating pressure is superimposed on constant external pressure, Fig. 2. Equation (22) has been evaluated for pulsating external pressure according to $p = p_o + \hat{p}\sin\omega t$, with frequency $\omega = 10^3$. The reduction of the critical time is indicated by the parameter $\hat{p}/p_c$. The initial imperfection $X_{oo} = 1.73$ has been assumed; e.g., fluctuations $\hat{p} = 0.2p_c$ superimposed on the mean value $p_o = 0.5p_c$ will reduce the critical time to about 30% of the critical time under constant external pressure $p_o = 0.5p_c$. As it may be calculated from Fig. 2, this corresponds just to the critical time under the constant external pressure $p_o = 0.6p_c$.

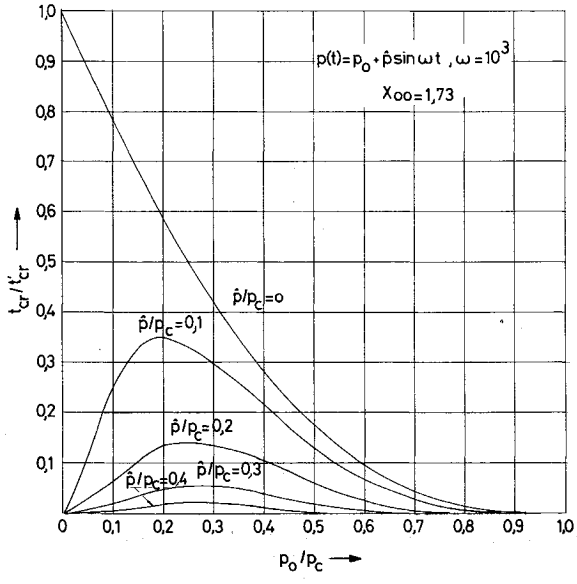

Fig. 2 Lifetime of a cylindrical shell under varying external pressure, $p(t) = p_o + \hat{p}\sin\omega t$, $\omega = 10^3$, $X_{oo} = 1.73$.

4) In particular, there exists a finite critical time for the symmetrically pulsating pressure $p = \hat{p}\sin\omega t$, $\hat{p} < p_c$, $0 \leqq t < t_{cr}$, although the pressure pulsates with frequency ω around the mean value zero, Fig. 2.

References

[1] Hoff, N. J., Jahsman, W. E., and Nachbar, W., "A Study of Creep Collapse of a Long Circular Cylindrical Shell Under Uniform External Pressure," *Journal of the Aerospace Sciences*, Vol. 26, No. 10, Oct. 1959, p. 663.

[2] Odqvist, F. K. G. and Hult, J., *Kriechfestigkeit metallischer Werkstoffe*, Springer, Berlin, 1962.

[3] Bargmann, H., "Kriechknicken bei veränderlicher Axiallast," *Ingenieur-Archiv*, Vol. 41, 1971, pp. 1–11.

Flight Test Base Pressure Results at Hypersonic Mach Numbers in Turbulent Flow

J. M. CASSANTO*
General Electric Company, King of Prussia, Pa.

Nomenclature

P_b	= base pressure
P_∞	= freestream pressure
P_b/P_∞	= base pressure ratio
M_∞	= freestream Mach number
M_L	= local cone Mach number preceding the base
P_L	= local cone pressure preceding the base
Re_L	= freestream Reynolds number based on length
r	= radius at any point on the base
R	= maximum base radius
$\dot{m}/\rho AV$	= mass addition parameter
α	= angle of attack

I. Introduction

FULL-SCALE flight vehicles (R/V's) generally have re-entry trajectories that produce Reynolds numbers which are an order of magnitude greater than the simulation capability of present ground test facilities. In addition, flight vehicles, in general, experience a fully turbulent boundary layer while in the hypersonic ($M_\infty \approx 20$) flight regime; this condition also cannot be simulated in present day ground test facilities. Accordingly, due to the preceding limitations, hypersonic base pressure data at high Reynolds numbers in turbulent flow are unavailable to the scientific community from ground test facilities.

The purpose of this Note is threefold: first, to present hypersonic ($M_\infty \approx 21$) full scale flight test base pressure data results for a low mass addition ($\dot{m}/\rho AV < .005$) slender cone having a fully turbulent boundary layer; second, to compare the present flight results with those of other investigators; and third, to show correlations of the combined data.

II. R/V Configuration, Instrumentation, Flight Conditions and Data Reduction

The GE R/V flight data presented in this paper are for a sharp 10° cone having a flat base. The heat shield consisted of an ablative material having low mass addition rates, $\dot{m}/\rho AV <$ 0.005.

Pressure instrumentation consisted of 0–0.10 psia and 0–1.0 psia pressure transducers located at various radii on the base. The present data were obtained with the 0–1.0 psia transducers located along a common ray at radial locations of $r/R = 0.3$, 0.5, and 0.67. The flight vehicle had a turbulent boundary layer during the data taking period based on transition data obtained with the low range (0–0.10 psia) base pressure sensors and calorimeters installed in the heat shield. In addition, the R/V had a nominal angle of attack on the order of a degree during the measurement period. The flight data were reduced only for that portion of the trajectory where the pressure sensors exceeded ten percent of full scale to insure data validity. The data were nondimensionalized to the form of base pressure to freestream pressure ratio utilizing a radar tracking trajectory and a measured atmosphere. It is estimated that the uncertainty band on the present measurements ranges from $\pm 30\%$ for the low Reynolds number data ($Re_L \approx 4 \times 10^7$) to $\pm 3\%$ for the high Reynolds number data ($Re_L \approx 2.5 \times 10^8$).

Presented as Paper 71-134 at the AIAA 9th Aerospace Sciences Meeting, New York, January 25–27, 1971; submitted February 4, 1971; revision received October 26, 1971. This work was partially supported under Air Force Contract AF 04(694)350.

Index categories: Launch Vehicle or Missile Flight Testing; Jets, Wakes, and Viscid-Inviscid Flow Interactions.

* Consulting Engineer, Aerodynamics Laboratory, Re-Entry and Environmental System Division. Member AIAA.

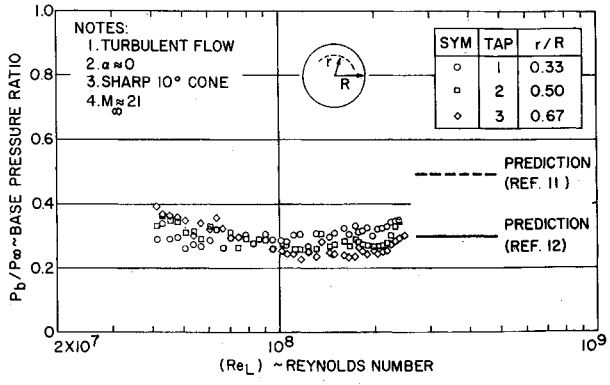

Fig. 1 Flight test base pressure data in turbulent flow for a sharp 10° cone.

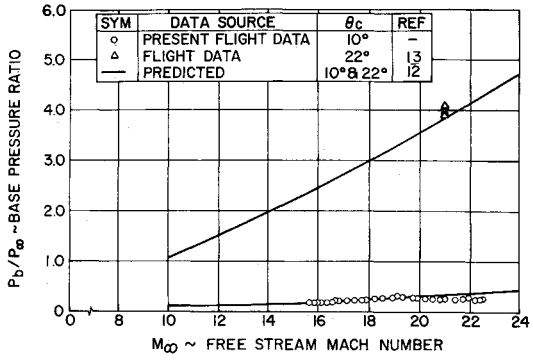

Fig. 3 Flight data showing the effect of cone angle and Mach number on base pressure ratio.

III. Flight Results

The present flight results are shown in Fig. 1 as a function of Reynolds number for the three pressure taps on the base. Several points are significant.

First, the base pressure ratio data can be seen to be relatively constant at $P_b/P_\infty \approx 0.3$ with Reynolds number, thus verifying the turbulent flow ground test data trends of Refs 1–7 and the theory of Ref. 8. This trend is in sharp contrast to laminar flow flight results,[9] which show that base pressure ratio can change by a factor of three with order of magnitude Reynolds number changes for off centerline pressure ports ($0.33 \leq r/R \leq 0.67$). Second, the apparent radial gradient trends between $Re_L \approx 4\times10^7 - 1\times10^8$ are not considered relevant or significant by the author since the pressure transducers are reading at the low end of their scale (where they are most inaccurate) and all the data points lie within the uncertainty error band of the sensors. However, $Re_L > 1\times10^8$ represents the threshold level where the data trends can be believed and these trends are considered relevant and significant since the difference between the readings of the pressure ports is greater than the uncertainty band of the data. This radial base pressure gradient trend (for $Re_L > 1\times10^8$) is qualitatively what would be expected (pressure decreasing with increasing base radius) for an ablative heat shield in turbulent flow, however, the magnitude of the gradient is greater than anticipated. The flight data show a gradient of approximately 30% (at $Re_L \approx 2\times10^8$) between a radial location of $r/R = 0.33$ to $r/R = 0.67$ while the predicted radial gradient[10] is approximately 10%.

Also shown for comparison with the flight data (Fig. 1) are the semiempirical predictions of Refs. 11 and 12. Reference 11 overpredicts the base pressure level by a considerable amount. This is because the technique, developed in 1965, was based heavily (80%) on a local flow correlation (see Fig. 4) of blunt body flight data. These flight data were all for low mass addition vehicles at small angles of attack. The bulk of the data when correlated were for local Mach numbers less than three corresponding with a freestream Mach number of twenty for blunt bodies. Only limited data were available at that time for higher local Mach numbers ($M_L \approx 10$) corresponding with freestream Mach numbers of 20 for slender (sharp) cones. Consequently, when a data fairing of the correlation was drawn, large uncertainties existed at the high local Mach number end of the correlation. Small errors in the local flow correlation produce large errors in the freestream base pressure as evidenced by the comparison shown in Fig. 1. The base pressure prediction technique was revised in 1968 (Ref. 12) to reflect limited ($M_\infty \approx 20$) sharp cone flight data for a similar configuration and lower Mach number ground test results. As observed, agreement with the present flight results is good.

Flight data showing the effect of Mach number on base pressure is presented in Fig. 2. Note that the flight data and the prediction technique (presented for comparison) are in basic agreement and show that base pressure ratio increases with increasing Mach number in the hypersonic flow regime. Cone angle and Mach number effects on base pressure are shown in Fig. 3 which compares the present GE 10° cone flight data with flight data for a 22° cone[13] and preflight predictions. Base pressure ratio can be seen to increase with increasing cone angle, as predicted.

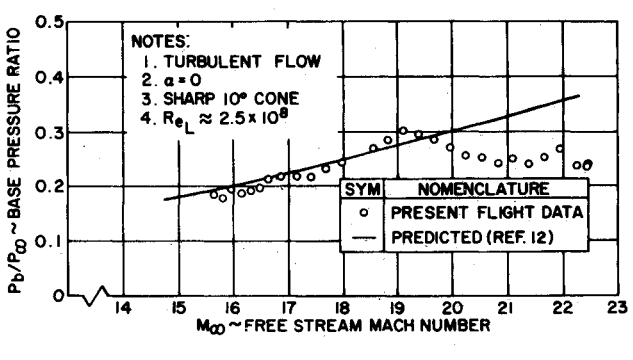

Fig. 2 Flight data showing the effect of Mach number on base pressure ratio.

IV. Data Correlation

The present flight results on the 10° cone and the 22° cone flight data[13] correlate well when the ratio of base to local cone pressure are plotted as a function of local Mach number preceding the base as shown in Fig. 4. Local flow conditions were computed from the cone tables and charts of Ref. 14. Also shown for comparison are the correlations of Refs. 11 and 12 based on earlier flight results previously discussed. Agreement is good which demonstrates that turbulent flow base pressure data for different configurations can be correlated if local flow conditions are utilized. The present data and unpublished flight data indicate that the original correlation[11] predicts base

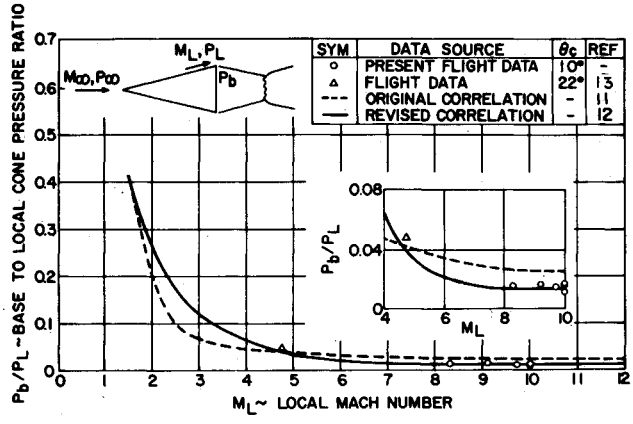

Fig. 4 Turbulent flow base pressure correlation.

pressure well for blunt bodies while the revised correlation[12] predicts base pressure best for sharp bodies.

References

[1] Chapman, D. R., "An Analysis of Base Pressure at Supersonic Velocities and Comparison with Experiment," Rept. 1051, 1951, NACA.

[2] Love, E. S., "Base Pressure at Supersonic Speeds on Two-Dimensional Airfoils and on Bodies of Revolution with and without Fins Having Turbulent Boundary Layers," TN 3819, Jan. 1957, NACA.

[3] Whitfield, J. D. and Potter, J. L., "On Base Pressures at High Reynolds Numbers and Hypersonic Mach Numbers," AEDC TN 60–61, March 1960, Arnold Engineering Development Center, Tullahoma, Tenn.

[4] Potter, J. L., Whitfield, J. D., and Strike, W. T., "Transition Measurements and the Correlation of Transition Sensitive Data," AEDC TR 59-4, Feb. 1959, Arnold Engineering Development Center, Tullahoma, Tenn.

[5] Cassanto, J. M., "Base Pressure Results at $M = 4$ Using Free-Flight and Sting-Supported Models," *AIAA Journal*, Vol. 6, No. 7, July 1968, pp. 1411–1414.

[6] Bogdonoff, S. M., "A Preliminary Study of Reynolds Number Effects on Base Pressure at $M = 2.95$," *Journal of Aeronautical Sciences*, Vol. 19, No. 3, March 1952, pp. 201–206.

[7] Kurzweg, H. H., "Interrelationship Between Boundary Layer and Base Pressure," *Journal of the Aeronautical Sciences*, Vol. 18, No. 11, Nov. 1951, pp. 743–748.

[8] Crocco, L. and Lees, L., "A Mixing Theory for the Interaction Between Dissipative Flows and Nearly Isentropic Streams," *Journal of the Aeronautical Sciences*, Vol. 19, No. 10, Oct. 1952, pp. 649–676.

[9] Cassanto, J. M., "Radial Base Pressure Gradients in Laminar Flow," *AIAA Journal*, Vol. 5, No. 12, Dec. 1967, pp. 2278–2279.

[10] Cassanto, J. M. and Hoyt, T. L., "Flight Results Showing the Effect of Mass Addition on Base Pressure," TIS 70SD248, March 1970, General Electric Company, Re-Entry and Environmental Systems Division, Philadelphia, Pa.; also *AIAA Journal*, Vol. 8, No. 9, Sept. 1970, pp. 1705–1707.

[11] Cassanto, J. M., "Effect of Cone Angle and Bluntness Ratio on Base Pressure," *AIAA Journal*, Vol. 3, No. 12, Dec. 1965, pp. 2351–2352.

[12] Cassanto, J. M. and Storer, E. M., "A Revised Technique for Predicting the Base Pressure of Sphere Cone Configurations in Turbulent Flow Including Mass Addition Effects," ALFM 68-41, Oct. 1968, General Electric Company, Re-Entry and Environmental Systems Division, Philadelphia, Pa.

[13] Sherman, M. M., and Nakamura, T., "Flight Test Measurements of Boundary Layer Transition on a Non-Ablating 22° Cone," *Journal of Spacecraft and Rockets*, Vol. 7, No. 2, Feb. 1970, pp. 137–142

[14] Ames Research Staff, "Equations, Tables, and Charts for Compressible Flow," Rept. 1135, 1953, NACA.

Laminar Thermal Boundary Layers on Continuous Surfaces

C. A. RHODES* AND H. KAMINER JR.†

University of South Carolina, Columbia, S. C.

Nomenclature

b = adiabatic wall temperature rise coefficient in Eq. (1)
c_p = specific heat at constant pressure
E = Eckert number $E = u_s^2/c_p(T_w - T_e)$
Nu = Nusselt number $Nu = hx/k$
Pr = Prandtl number $Pr = c_p\mu/k$
Re = Reynolds number $Re = u_s x/\nu$
T = temperature
T_e = freestream temperature
T_w = wall temperature
u = velocity component in x direction
u_s = surface velocity
x = coordinate parallel to surface
y = coordinate normal to surface
η = dimensionless coordinate $\eta = y(u_s/\nu x)^{1/2}$
θ_1 = dimensionless temperature $\theta_1 = (T - T_e)/(T_w - T_e)$
θ_2 = dimensionless temperature, adiabatic wall
μ = absolute viscosity
ν = kinetic viscosity

Received May 19, 1971; revision received September 21, 1971.

Index categories: Boundary Layers and Convective Heat Transfer—Laminar; Shock Waves and Detonation; Hydrodynamics.

* Associate Professor of Engineering, College of Engineering. Member AIAA.

† Undergraduate Student.

Introduction

THE boundary layer on a continuous surface is the flow situation where a plane surface moves from a wall into a quiescent fluid. This situation occurs in the extrusion of films and plates. It has also been shown that the same boundary-layer conditions occur on surfaces behind shock waves transverse to a surface and moving parallel to it such as in a shock tube. Mirels[1] first considered compressible flow in boundary layers behind shock waves while Sakiadis[2,3,4] considered incompressible flow on continuous surfaces. Other studies have been made and a number of these are contained in Refs. 5–12.

This Note presents comparisons between the heat-transfer characteristics of the continuous surface with those of the semi-infinite plate with constant freestream velocity and laminar flow. The data for flow over a semi-infinite flat plate used to compare with continuous surface results were obtained from Schlichting[13] and Kays.[14] These comparisons are performed for Prandtl numbers in the region from 0.1 to 1000. Heat-transfer characteristics are compared for constant wall temperature, uniform wall heat flux, and adiabatic wall with viscous dissipation. These results are applicable to incompressible fluids with constant properties and compressible fluids which are ideal gases with viscosity proportional to temperature.

Analysis

The boundary-layer equations for a continuous surface were reduced to their similarity form by Mirels[1] and for the sake of brevity will not be reproduced here. In the present analysis, we consider only the case of zero freestream velocity. Two-dimensional boundary layers are considered and steady flow assumed. The analysis was performed on a digital computer by numerical integration of these equations utilizing the Runge-Kutta technique.

Results

The heat-transfer coefficient, assuming viscous dissipation can be neglected, was determined for both uniform wall temperature and uniform wall heat flux. These results are contained in Fig. 1 where $Nu/(RePr)^{\frac{1}{2}}$ is plotted as a function of Prandtl number.

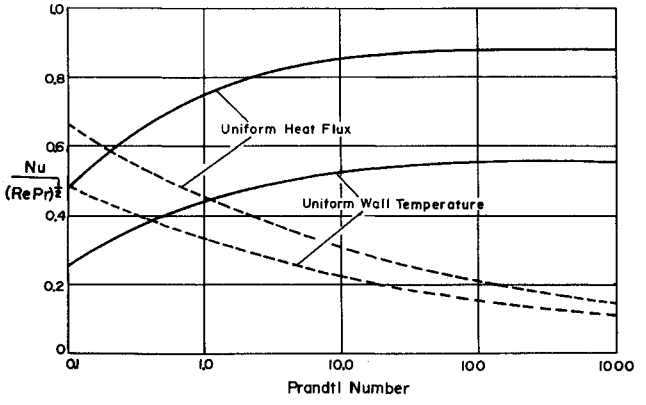

Fig. 1 Heat-transfer coefficient, $Nu/(RePr)^{\frac{1}{2}}$, as a function of Prandtl number. Solid line is continuous surface and dashed line is semi-infinite flat plate.